FUNCTIONAL ROLE OF *OPN* AND *LGMN* IN B-CELL ACUTE LYMPHOBLASTIC LEUKEMIA (B-ALL)

#SANTORO, J.C.[1#], BASTOS, A.C.[2], BRUM, M.C.M.[2], ABDO, L.[3], PRETTI, M.A.[3], BONAMINO, M.H.[3], GIMBA, E.R.[2'4], EMERENCIANO, M.[1]

[1]Molecular Cancer Study group, Division of Clinical Research, Research Center, INCA, RJ, Brazil

[2]Group of Structural and Molecular Oncobiology, Cell Biology Program, Research Center, INCA, RJ, Brazil

[3]Molecular Carcinogenesis Program, Research Center, INCA-RJ, Brazil [4]Department of Nature Sciences, IHS, UFF, RJ, Brazil

Abstract

Introduction: B-cell acute lymphoblastic leukemia (B-ALL) not otherwise specified, also known as "B-other" are associated with intermediate prognosis and high risk of relapse. This B-ALL subtype is characterized by the absence of recurrent genetic abnormalities. Relapse is associated with a dismal prognosis. Studies suggest biological mechanisms that may contribute to chemoresistance (CR) and increased risk of relapse in B-ALL. Osteopontin (*OPN*) has been shown to be differentially expressed in B-ALL and is associated with isolated central nervous system (CNS) relapses. In addition, increased levels of legumain (*LGMN*) have been reported in B-ALL with CNS infiltration. **Objective**: Our objective was to assess whether *OPN* and *LGMN* deregulation is correlated with CR mechanisms in B-other ALL. **Methods:** Cell line 207, established from a relapsed of B-ALL without recurrent genetic abnormalities, was used as *in vitro* model of B-other ALL. RS4;11 t(4;11) and REH t(12;21) cell lines were used forcomparison. Gene expression of *LGMN, OPN* (and splicing variants) and genes related to adhesion, invasion, metastasis and drug efflux (*CD44s, TWIST1, SNAI2, VIM* and *PgP*) were evaluated by RT-qPCR. DNA oligomers and siRNAs were used to silence LGMN and OPN. Functional assays were performed to evaluate participation of *LGMN* and *OPN* in CR mechanisms (adhesion, dormancy and sensitivity to vincristine, VCR, and etoposide, VP-16). 207 cells were cultured under low serum conditions to induce dormant cell. **Results:** Increased mRNA levels of *OPN* and *LGMN* were observed in 207 versus RS4;11 (LGMN p=0.0325) and REH (OPN p=0.0025; LGMN p=0.0347). OPNc was the variant with highest mRNA levels in 207. Single silencing of OPN, OPNc or LGMN was associated with reduced mRNA of genes: *OPN* (*CD44s* p=0.0024, *TWIST1* p<0.0001), *OPNc* (*CD44s* p=0.0072, *TWIST1* p=0.0183, *SNAI2* p=0.0221, *VIM* p=0.0298, PgP p=0.0233) and *LGMN* (*VIM* p=0.0073). Total *OPN* and *OPNc* knockdown reduced mRNA levels of *LGMN* (*OPN* p=0.0153, *OPNc* p=0.0430). Cell dormancy was confirmed by increased expression of *DYRK1A* (48h p=0.0331). After induction dormancy were observed higher mRNA levels of OPN (72h p=0.0030), OPNc (48h p=0.0033), *LGMN* (24h p=0.0078), *CD44s* (24h p=0.0056; 48h p=0.0190; 72h p=0.0299), *E-cad* (48h p=0.0069; 72h p=0.0462) and PgP (24hp=0.0304). In addition, were observed resistance to *VCR* and *VP-16* (VCR 24h p=0.0016 and 48h p=0.0004, *VP-16* 48h p=0.0044)with increased *mRNA* levels of *OPNc* (VCR 48h p=0.0054) and PgP (VP-16 48h p=0.0462). After 24h of exposure to VCR and VP-16 were observed higher mRNA levels of OPNc (VCR p=0.0423), *LGMN* (VCR p=0.0413) and PgP (VCR p=0.0415, VP-16p<0.0001). *OPNc* knockdown induced increased sensitivity to VCR and VP-16 (24h VCR p=0.0397; 72h p=0.0246; VP-16 48h p=0.0177). **Conclusion:** Our data show that *OPN*, notably *OPNc*, and *LGMN* are involved in mechanisms

Hypothesis:

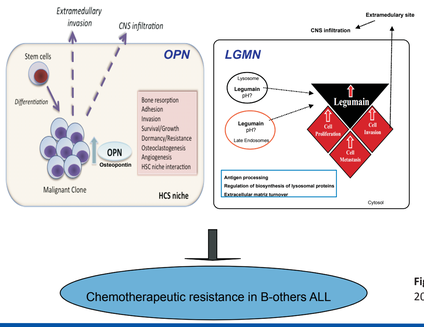

Figure 1. Hypothesis (Modified from BASTOS *et al*, 2017; DALL; BRANDSTETTER, 2016)

Methods

Experimental design

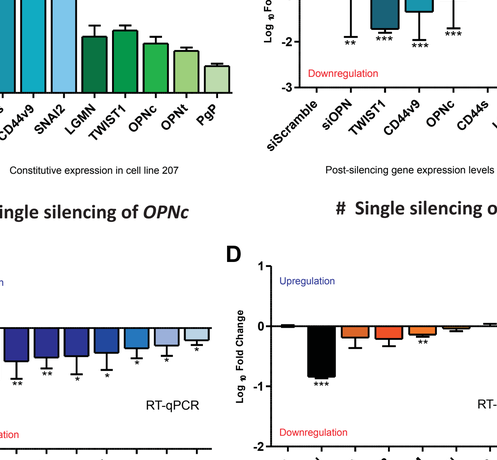

Figure 2. Study flowchart

Results

Constitutive gene expression analysis

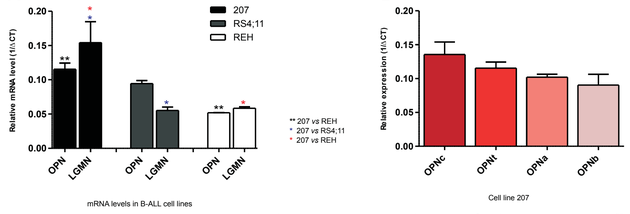

Figure 3. mRNA levels in B-ALL cell lines. **A.** Higher levels mRNA of *OPN* and *LGMN* were observed in 207 vs REH and RS4;11 cell lines, respectively. **B.** *OPNc* was the variant with highest mRNA levels in 207 cells. 207: (without recurrent genetic abnormalities), REH (*ETV6-RUNX1* fusion), RS4;11 (MLL gene rearrangements) *P < 0.05; **P < 0.01 (Student's t-test).

Constitutive gene expression analysis

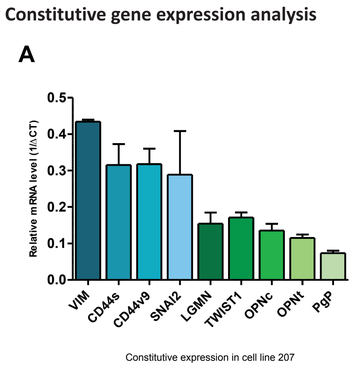

Single silencing of *OPN*

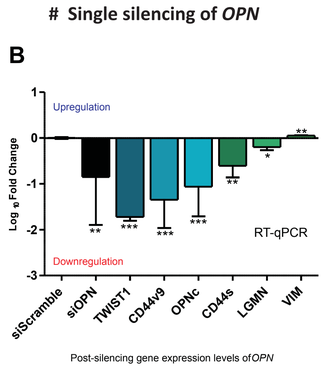

Single silencing of *OPNc*

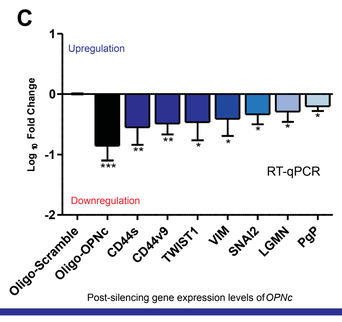

Single silencing of *LGMN*

Figure 4. mRNA levels in cell line 207. **A.** Constitutive gene expression in cell line 207. **B**. Single silencing of OPN was associated with reduced mRNA of genes *TWIST1, CD44v9, CD44s, OPNc, LGMN* and *OPN*. **C.** Single silencing of OPNc was associated with reduced mRNA of genes *CD44s, CD44v9, TWIST1, VIM, SNAI2, LGMN* and *PgP*. **D.** Single silencing of *LGMN* was associated with reduced mRNA of genes *CD44s, SNAI2, VIM* and mRNA levels of TWIST1 *P < 0.05; **P < 0.01 (Student's t-test).

mRNA levels and cell adhesion after *OPNc* silencing

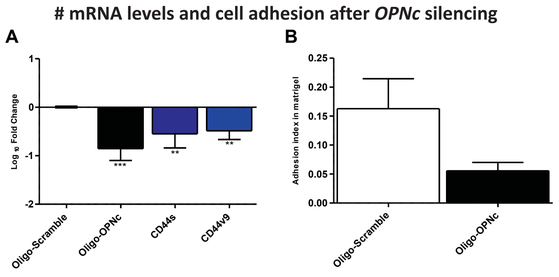

Figure 5. mRNA levels and cell adhesion after *OPNc* silencing in cell line 207. **A**.Single silencing OPNc reduced mRNA levels of *CD44s* and *CD44v9* adhesion markers. **B**. Adhesion matrix capacity of 207 cell line with *OPNc* knockdown in comparison to scramble *P < 0.05; **P < 0.01 (Student's t-test).

Cell proliferation inhibition by FBS reduction (Cell dormancy)

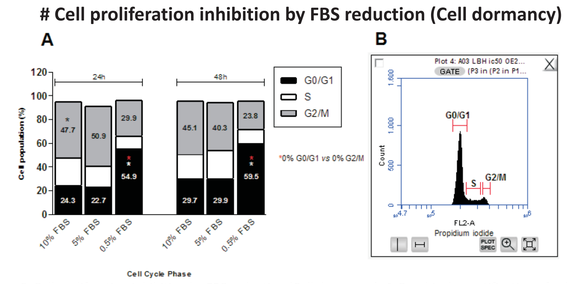

Figure 6. Cell proliferation inhibition by FBS reduction (Cell dormancy). **A**.Graphical quantification of cell cycle phases. **B**. Cell cycle analysis using propidium iodide (PI) staining and flow cytometry. *P < 0.05; **P < 0.01 (Student's t-test).

Post-cellular dormancy mRNA levels in cell line 207

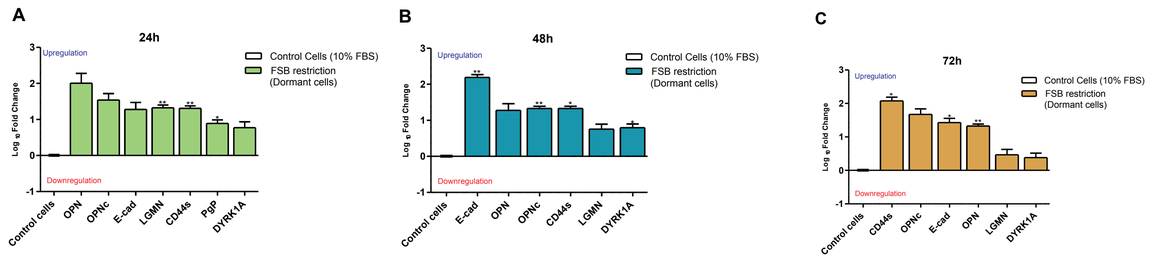

Figure 7. Post-cellular dormancy mRNA levels in cell line 207. **A.** mRNA levels after 24 hours of FBS deprivation. **B.** mRNA levels after 48 hours of FBS deprivation. **C.** mRNA levels after 72 hours of FBS deprivation *P < 0.05; **P < 0.01 (Student's t-test).

Cell viability (IC50) and mRNA levels after drugs treatment

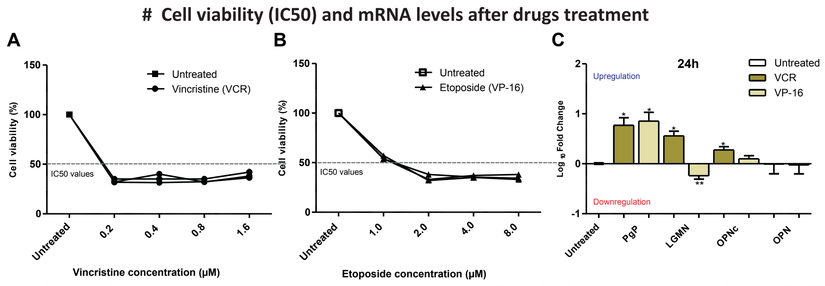

Figure 8. Cell viability assay to determine the IC50 value of vincristine (VCR) and etoposide (VP-16) and mRNA levels after drugs treatment in B-ALL cell line 207.The different drug concentrations used and the corresponding cell viability graphs are shown for VCR **(A)** and VP-16 **(B)**. Cells were exposed to VCR (0 at 1.6 μM) and VP-16 (0 at 8 μM) for 48 h and cell viability was measured by MTT assay. **(C).** mRNA levels after drugs treatment in B-ALL cell line 207 by RT-qPCR (24h) *P < 0.05; **P < 0.01 (Student's t-test).

Cell viability of dormant cells after drugs treatment

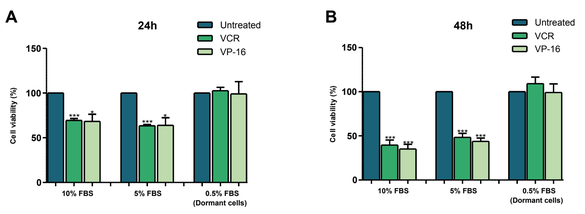

Figure 9. Cell viability of dormant cells after drugs treatment. **A**. Increased dormant cell drug resistance after VCR and VP-16 treatment by MTT assay (24h) and **B**. (48h).*P < 0.05; **P < 0.01 (Student's t-test).

Cell viability of 207 cells after *OPN* silencing

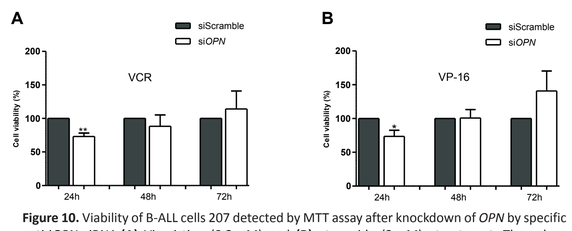

Figure 10. Viability of B-ALL cells 207 detected by MTT assay after knockdown of *OPN* by specific anti-i*OPN* siRNA.**(A)** Vincristine (0.2 μM) and **(B)** etoposide (2 μM) treatment. The values represent means ± SD of three cultures from triplicate-independent experiments. *p<0.05 by Student's t-test

Cell viability of 207 cells after *OPNc* silencing

Figure 11. Viability of B-ALL cells 207 detected by MTT assay after knockdown of *OPNc* by specific anti-*OPNc* phosphorotiothate-modified DNA oligomers.**(A)** Vincristine (0.2 μM) and **(B)** etoposide (2 μM) treatment. The values represent means ± SD of three cultures from triplicate-independent experiments. *p<0.05 by Student's t-test

Conclusion

Our data show that *OPN*, notably *OPNc*, and *LGMN* are involved in mechanisms that can mediate CR to leukaemic drug treatment, such as adhesion, dormancy, drug efflux and invasion to extramedullary sites.

Figure 12. Clonal evolution of leukemic cells from preleukemic stage to relapse (Modified from GAUDICHON *et al*., 2019)

[1]VELDEN et al., 2015
[2]STREFFORD et al., 2006

Projeto Gráfico: Área de Edição e Produção de Materiais Técnico-Científicos / INCA

Financial support

CAPES FAPERJ CNPq INCA SUS MINISTÉRIO DA SAÚDE PÁTRIA AMADA BRASIL GOVERNO FEDERAL